

Semiexclusive dilepton production in proton-proton collisions with one forward proton measurement at the LHC

Barbara Linek

E-Mail: barbarali@dokt.ur.edu.pl

College of Natural Sciences, Institute of Physics, University of Rzeszów, ul. Pigonia 1, PL-35-959 Rzeszów, Poland

Presented at the Low- x Workshop, Elba Island, Italy, September 27–October 1 2021

We discuss the mechanisms of photon-photon fusion triggering the dilepton production in proton-proton collisions with rapidity gap in the main detector and one forward proton in the forward proton detectors. This correspond to the LHC measurements made by ATLAS+AFP and CMS+PPS. Transverse momenta of the intermediate photons and photon fluxes expressed by the form factors and structure functions are included. Moreover the influence of proton measurement and cuts on the $\xi_{1/2}$, M_{ll} , Y_{ll} , $p_{t,ll}$ distributions, cross section and gap survival factor are considered for both double-elastic and single-dissociative processes.

The analyzes used the SuperChic generator to calculate the soft gap survival factor and to compare the results obtained with its use to the results obtained on the owned codes available. It is shown that the gap survival factor for the single dissociative mechanism is related to the emission of a (mini)jet into the main detector depending on the type of contribution. The dependence between this value and the invariant mass as well as the transverse momentum of the leptons pair and its rapidity was also found.

1 Introduction

The photon-photon fusion is one of the dilepton production mechanism in proton-proton collisions, that was measured recently by the CMS [1] and ATLAS [2] collaborations for the cases with one proton measurement in forward direction. A description of the codes created by our group that enables the analysis of such processes is included in [3–5]. This is the basis of our formalism to include the gap survival factor associated with the emission of (mini) jets for the production of W^+W^- [6], $t\bar{t}$ [7] and $\mu^+\mu^-$ [8]. However, it is necessary to apply the kinematic condition to the ξ -variables (longitudinal momentum fraction loss) in order to compare the theoretical data with the experimental results [1, 2]. The results of the research from the last mentioned work are presented in this article.

This analysis is related to the three types of photon initiated events shown in Fig.1. There are double elastic and two types of single dissociation processes. The analysis of the mentioned

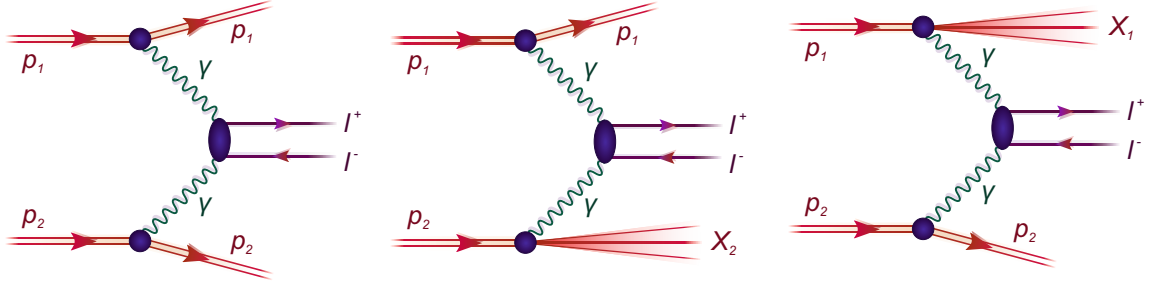


Figure 1: Three different categories of $\gamma\gamma$ fusion mechanisms of dilepton production in proton-proton collisions.

processes is performed with the use of k_T -factorization approach in which the cross-section for l^+l^- is described as:

$$\frac{d\sigma^{(i,j)}}{dy_1 dy_2 d^2\mathbf{p}_1 d^2\mathbf{p}_2} = \int \frac{d^2\mathbf{q}_1}{\pi\mathbf{q}_1^2} \frac{d^2\mathbf{q}_2}{\pi\mathbf{q}_2^2} \mathcal{F}_{\gamma^*/A}^{(i)}(x_1, \mathbf{q}_1) \mathcal{F}_{\gamma^*/B}^{(j)}(x_2, \mathbf{q}_2) \frac{d\sigma^*(p_1, p_2; \mathbf{q}_1, \mathbf{q}_2)}{dy_1 dy_2 d^2\mathbf{p}_1 d^2\mathbf{p}_2}, \quad (1.1)$$

where the indices $i, j \in \{\text{el}, \text{in}\}$ denote elastic or inelastic final states. Here the photon flux for inelastic case is integrated over the mass of the remnant.

The longitudinal momentum fractions of photons are obtained from the rapidities and transverse momenta of final state l^+l^- as:

$$\begin{aligned} x_1 &= \sqrt{\frac{\mathbf{p}_1^2 + m_l^2}{s}} e^{+y_1} + \sqrt{\frac{\mathbf{p}_2^2 + m_l^2}{s}} e^{+y_2}, \\ x_2 &= \sqrt{\frac{\mathbf{p}_1^2 + m_l^2}{s}} e^{-y_1} + \sqrt{\frac{\mathbf{p}_2^2 + m_l^2}{s}} e^{-y_2}. \end{aligned} \quad (1.2)$$

The integrated fluxes for elastic and inelastic processes are expressed for the elastic case by the proton electromagnetic form factor, while the inelastic flux is expressed by the proton structure function $F_2(x_{Bj}, Q^2)$ and $F_L(x_{Bj}, Q^2)$ [4, 5]:

$$\begin{aligned} \mathcal{F}_{\gamma^* \leftarrow A}^{\text{el}}(z, \mathbf{q}) &= \frac{\alpha_{\text{em}}}{\pi} \left[(1-z) \left(\frac{\mathbf{q}^2}{\mathbf{q}^2 + z(M_x^2 - m_A^2) + z^2 m_A^2} \right)^2 \frac{4m_p^2 G_E^2(Q^2) + Q^2 G_M^2(Q^2)}{4m_p^2 + Q^2} \right], \\ \mathcal{F}_{\gamma^* \leftarrow A}^{\text{in}}(z, \mathbf{q}) &= \frac{\alpha_{\text{em}}}{\pi} \left[(1-z) \left(\frac{\mathbf{q}^2}{\mathbf{q}^2 + z(M_x^2 - m_A^2) + z^2 m_A^2} \right)^2 \frac{F_2(x_{Bj}, Q^2)}{Q^2 + M_x^2 - m_p^2} \right]. \end{aligned} \quad (1.3)$$

Then the four-momenta of intermediate photons are written as:

$$\begin{aligned} q_1 &\approx \left(x_1 \frac{\sqrt{s}}{2}, \vec{q}_{1t}, x_1 \frac{\sqrt{s}}{2} \right), \\ q_2 &\approx \left(x_2 \frac{\sqrt{s}}{2}, \vec{q}_{2t}, -x_2 \frac{\sqrt{s}}{2} \right). \end{aligned} \quad (1.4)$$

There is non-zero probability of a proton emission from the remnant system. The analysis of this requires modeling of remnant fragmentation. ξ for this type of processes is more than 0.1 therefore, the measurement in the Roman pots of the ATLAS or CMS experiments is not possible. This condition can be only met by the diffractive mechanism shown in the Fig.2.

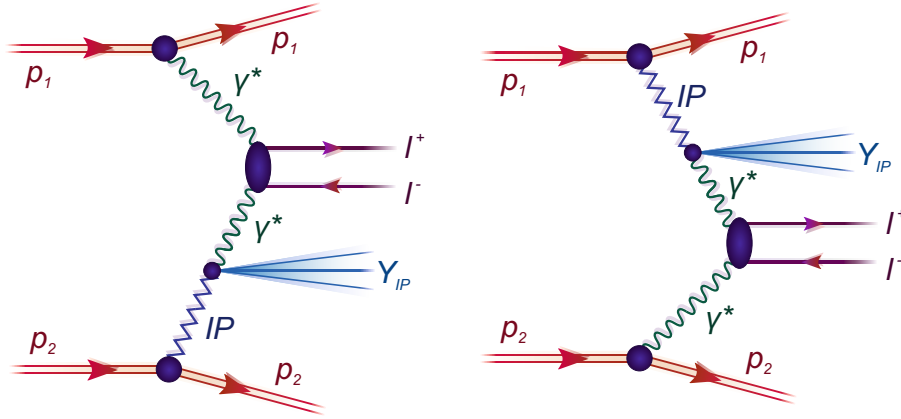


Figure 2: Diffractive mechanisms of dilepton production in proton-proton collisions.

Comparing the theoretical data with the experimental results requires the imposition of the ξ -variables, that is calculated by ATLAS analysis as:

$$\xi_1 = \xi_{ll}^+, \quad \xi_2 = \xi_{ll}^- . \quad (1.5)$$

The longitudinal momentum fractions of the photons were calculated by them as:

$$\begin{aligned} \xi_{ll}^+ &= (M_{ll}/\sqrt{s}) \exp(+Y_{ll}) , \\ \xi_{ll}^- &= (M_{ll}/\sqrt{s}) \exp(-Y_{ll}) . \end{aligned} \quad (1.6)$$

The above formula was also used in the discussed analyzes however, only lepton variables are entered in it.

2 Results

In the calculations described below we shall take typical cuts on dileptons: $-2.5 < y_1, y_2 < 2.5$, $p_{1t}, p_{2t} > 15$ GeV and extra cuts on ξ_{ll}^+ or ξ_{ll}^- . The results from SuperChic [9] and from our codes are similar, therefore they are not duplicated. All results are available in [8].

In Fig.3 the distribution in dimuon invariant mass for the case without ξ cuts (left panel) and with ξ cuts (right panel) are presented. The elastic-elastic (dashed line) and elastic-inelastic + inelastic-elastic (solid line) are shown separately. On average larger invariant masses in the case with ξ cuts are observed.

The Fig.4 presents similar distributions but in Y_{ll} . Without the ξ cut quite different shapes of distributions in Y_{ll} without and with soft rapidity gap survival factor (see the left panel) can be observed. When the ξ -cut is imposed, the distributions with and without soft rapidity gap survival factor have very similar shapes. Then, however, the elastic-inelastic and inelastic-elastic contributions are well separated in Y_{ll} . The sum of both contributions has a characteristic dip at $Y_{ll} = 0$.

The Fig.5 shows corresponding gap survival factor calculated as:

$$S_G(M_{ll}) = \frac{d\sigma/dM_{ll}|_{withSR}}{d\sigma/dM_{ll}|_{withoutSR}} , \quad (2.1)$$

$$S_G(p_{t,pair}) = \frac{d\sigma/dp_{t,pair}|_{withSR}}{d\sigma/dp_{t,pair}|_{withoutSR}} . \quad (2.2)$$

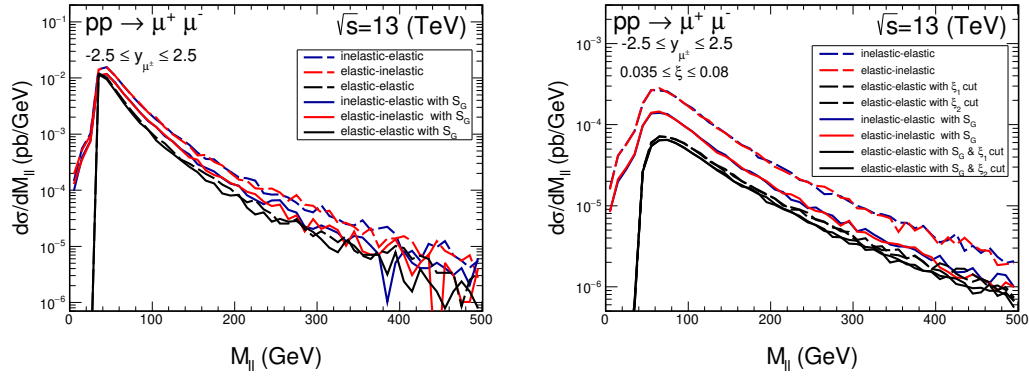


Figure 3: Distribution in dimuon invariant mass for the different contributions considered. We consider the case without ξ cuts (left panel) and with ξ cuts (right panel).

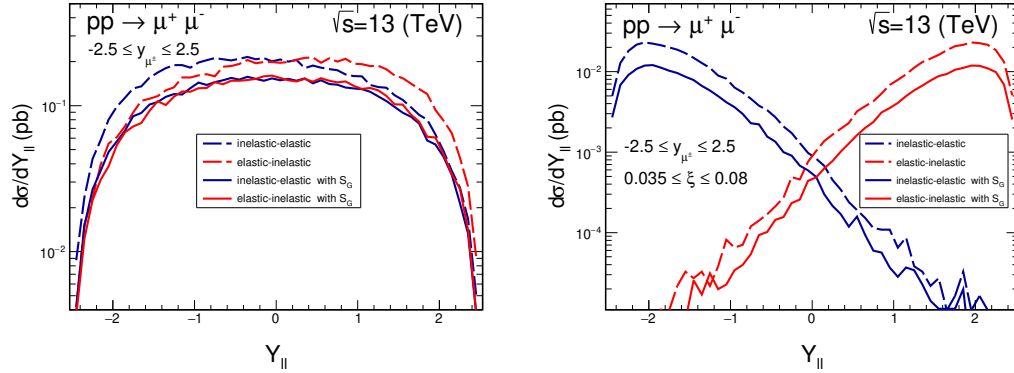


Figure 4: Distribution in rapidity of the dimuon pair. We show the case without ξ cuts (left panel) and with ξ cuts (right panel). for the different contributions considered.

The ratio of the cross section with the soft rapidity gap survival factor to its counterpart without including the effect was calculated, the difference is visible in M_{ll} (left panel) or in $p_{t,pair}$ (right panel) for double elastic (dashed line) and single dissociation (solid line). A small dependence on both M_{ll} and on $p_{t,pair}$ can be observed here. The gap survival factor for double elastic component is larger than for single dissociation and the gap survival factor corresponding to the measurement of one proton is significantly smaller than that for the inclusive case. The rather large fluctuations are due to limited statistics (50 000 events).

The Fig.6 shows in addition soft gap survival factor as a function of the rapidity of the dimuon pair. A strong dependence of the gap survival factor on Y_{ll} separately for elastic-inelastic and inelastic-elastic components can be observed but only in the case when proton is not measured. This effect may be very difficult to address experimentally as in this (no proton measurement) case one measures the sum of the both (all) components, where the effect averages and becomes more or less independent of Y_{ll} (see black dash-dotted curve). However, it seems interesting to understand the dependence on Y_{ll} for individual component from theoretical point of view.

The fact how the proton dissociation further reduces the gap survival factor due to emission of a (mini)jet that can enter into the main detector and destroy the rapidity gap is also interesting.

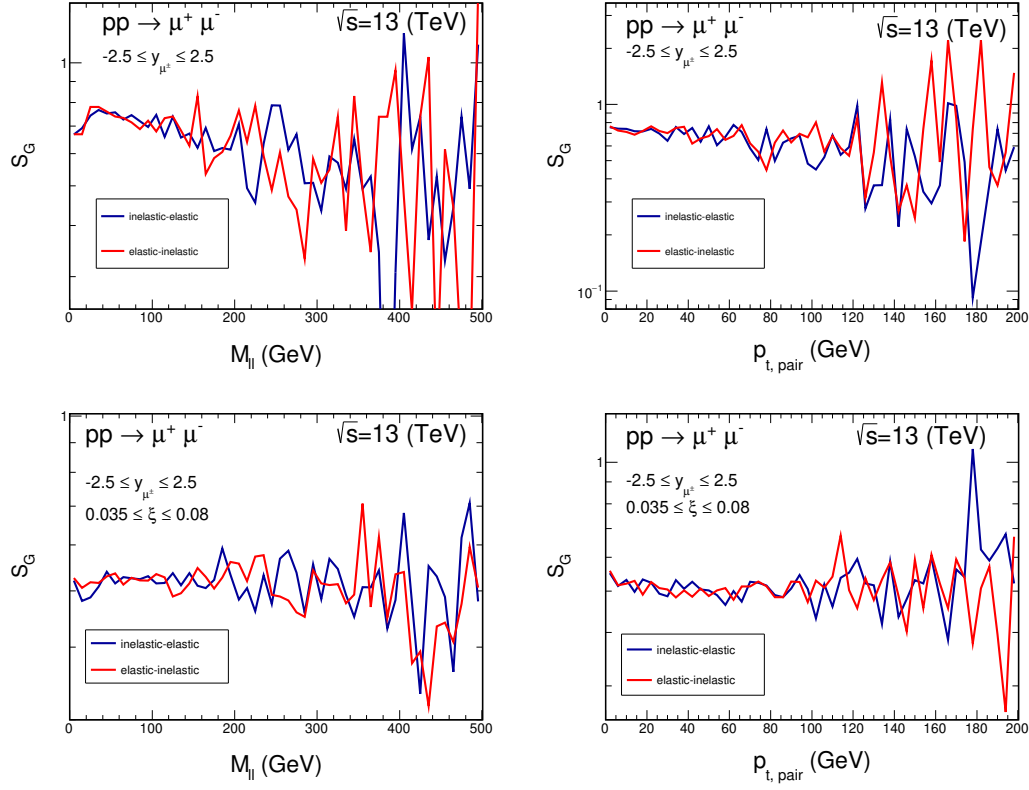


Figure 5: The soft gap survival factor as a function of dilepton invariant mass (left panels) and as a function of transverse momentum of the pair (right panels) for single dissociation (solid line) mechanisms. We show the result without ξ cuts (upper panels) and with ξ cuts (lower panels).

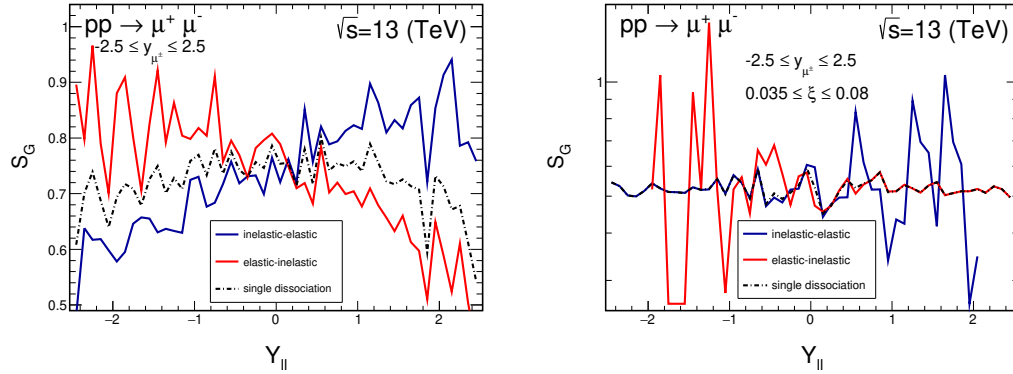


Figure 6: The soft gap survival factor as a function of rapidity of the $\mu^+ \mu^-$ pair for single proton dissociation. We show the result without ξ cuts (left panel) and with ξ cuts (right panel). The dash-dotted black line represents effective gap survival factor for both single-dissociation components added together.

This was discussed e.g. in [5, 7, 10]. In Fig.7 the (mini)jet distribution in rapidity for elastic-inelastic and inelastic-elastic components are shown without imposing the ξ cut (left panel) and

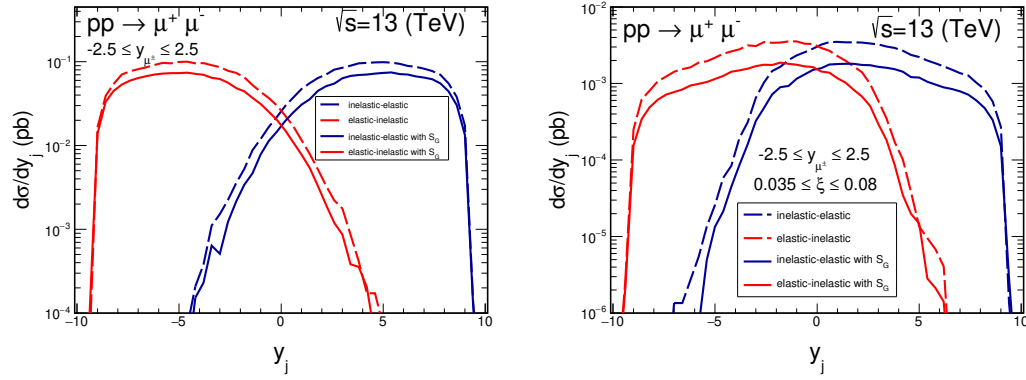


Figure 7: Distribution in the (mini)jet rapidity for the inclusive case with no ξ cut (left panel) and when the cut on ξ is imposed (right panel) for elastic-inelastic and inelastic-elastic contributions as obtained from the SuperChic generator. We show result without (dashed line) and with (solid line) soft rescattering correction.

Table 1: Gap survival factor due to minijet emission. The first block is with only internal SuperChic cut: $-2.5 < Y_{ll} < 2.5$, the second block is when the condition on individual rapidities is imposed extra, the third block includes in addition the cut on ξ_1 or ξ_2 , and the final block includes also the condition $p_{t,pair} < 5$ GeV. In all cases $p_{1t}, p_{2t} > 15$ GeV. In the last panel (*) means 10 000 events only.

contribution	without S_G	with S_G
cut on Y_{ll} only		
elastic-inelastic	0.76304	0.78756
inelastic-elastic	0.76278	0.78898
cut on y_1 and y_2 in addition		
elastic-inelastic	0.77366	0.79250
inelastic-elastic	0.76926	0.78744
cut on ξ_1 or ξ_2 in addition		
elastic-inelastic	0.52430	0.53976
inelastic-elastic	0.53118	0.53614
cut on $p_{t,pair}$ in addition		
elastic-inelastic	0.83144	0.84350(*)
inelastic-elastic	0.83462	0.84960(*)

when imposing the ξ cut (right panel). One can observe slightly different shape for both cases. The corresponding gap survival factor (probability of no jet in the main detector) is 0.8 and 0.5, respectively. The probability of no emission around the $\gamma\gamma \rightarrow \mu^+\mu^-$ vertex is, however, much more difficult to calculate and requires inclusion of remnant hadronization which is model dependent.

In Table I the probability that the (mini)jet is outside the main detector, i.e.: $y_{jet} < -2.5$ or $y_{jet} > 2.5$ is shown. Imposing cuts on ξ lowers the corresponding (mini)jet rapidity gap survival factor while imposing extra cut $p_{t,pair} < 5$ GeV, as in the ATLAS experiment, increases it back.

The factor below is included in the case when rapidity gap condition is imposed experimentally. It is less clear what to do when the condition of separated μ^+ and μ^- are imposed as in the ATLAS experiment [2]. In the following it is assumed that the particles from (mini)jet, emitted from the same vertex as leptons, will always break the conditions, provided they are emitted in the

same range of rapidities as the measured leptons. This range is defined by the geometry of the main ATLAS (CMS) detector.

3 Conclusions

These proceedings discuss the production of dileptones initiated by a photon-photon fusion with one forward proton measurement. Conditions on ξ_1 or ξ_2 for the forward emitted protons were imposed therein. Particular interesting is the distribution in M_{ll} and in Y_{ll} which has a minimum at $Y_{ll} \approx 0$. Several distributions were discussed in [8].

The soft rapidity gap survival factor was calculated as a function of M_{ll} , $p_{t\text{pair}}$ and Y_{ll} . There are no obvious dependences on the variables have been found for the single dissociation, except of distribution in Y_{ll} , however there is a strong dependence on the proton measurement.

There was also calculated gap survival factor due to (mini)jet emission by checking whether the (mini)jet enters to the main detector or not. This type of gap survival also strongly depends on the outgoing proton is measurement or not. It is about 0.8 for inclusive case and about 0.5 for the case with proton measurement in forward proton detector.

References

- [1] A.M. Sirunyan et al. (CMS Collaboration), JHEP07 (2018) 153.
- [2] G. Aad et al. (ATLAS collaboration), Phys. Rev. Lett. **125**, 261801 (2020), arXiv:2009.14537.
- [3] G.G. da Silva, L. Forthomme, K. Piotrkowski, W. Schäfer and A. Szczurek, JHEP **02** (2015) 159, arXiv:1409.1541.
- [4] M. Łuszczak, W. Schäfer and A. Szczurek, Phys. Rev. **D93** (2016) 074018.
- [5] M. Łuszczak, W. Schäfer and A. Szczurek, JHEP **05** (2018) 064.
- [6] L. Forthomme, M. Łuszczak, W. Schäfer and A. Szczurek, Phys. Lett. **B789** (2019) 300.
- [7] M. Łuszczak, L. Forthomme, W. Schäfer and A. Szczurek, JHEP **02** (2019) 100.
- [8] A. Szczurek, B. Linek and M. Łuszczak, Phys. Rev. **D104** 074009 (2021), arXiv:2107.02535.
- [9] L.A. Harland-Lang, M. Tasevsky, V.A. Khoze and M.G. Ryskin, Eur. Phys. **C80** (2020) 925, arXiv:2007.12704.
- [10] L.A. Harland-Lang, V.A. Khoze and M.G. Ryskin, Eur. Phys. J. **C76** (2016) 255, arXiv:1601.03772.